Materials Research Express

CrossMark

OPEN ACCESS

RECEIVED
11 December 2024

REVISED
26 December 2024

ACCEPTED FOR PUBLICATION
2 January 2025

PUBLISHED
10 January 2025

PAPER

Modification of surface and subsurface properties of cold-rolled Ti6Al4V sheets through water jet shot peening

Egemen Avcu[1,2], Mustafa Armağan[3], Yasemin Yıldıran Avcu[2], Eray Abakay[4], Emirhan Çalım[2,5], Funda Gül Koç[6], Mert Guney[7,8] and Rıdvan Yamanoğlu[6]

[1] Machine and Metal Technologies, Ford Otosan Ihsaniye Automotive Vocational School, Kocaeli University, Kocaeli, 41650, Turkiye
[2] Department of Mechanical Engineering, Engineering Faculty, Kocaeli University, Kocaeli, 41380, Turkiye
[3] Department of Mechanical Engineering, Faculty of Engineering and Natural Sciences, Istanbul Medeniyet University, Istanbul, 34700, Turkiye
[4] Department of Metallurgy and Materials Engineering, Engineering Faculty, Sakarya University, Sakarya, 54050, Turkiye
[5] Department of Mechanical Engineering, Engineering Faculty, Piri Reis University, Istanbul, 34940, Turkiye
[6] Department of Metallurgy and Materials Engineering, Engineering Faculty, Kocaeli University, Kocaeli, 41380, Turkiye
[7] The Environment and Resource Efficiency Cluster (EREC), Nazarbayev University, Astana, 010000, Kazakhstan
[8] Department of Civil and Environmental Engineering, Nazarbayev University, Astana, 010000, Kazakhstan

E-mail: avcuegemen@gmail.com

Keywords: strain hardening, deformation, ANOVA, titanium alloys, tribological behaviour, surface modification

Abstract

Titanium alloys possess remarkable properties, such as high strength, biocompatibility, and resistance to corrosion. Nonetheless, both their surface and subsurface properties require improvements, particularly for applications where surface contact is unavoidable. The present study utilises an emerging mechanical surface treatment technique (water jet shot peening) for modifying the surface and subsurface characteristics of cold-rolled Ti6Al4V sheets. Water jet shot peening was applied on Ti6Al4V samples following an L18 full factorial experimental design, focusing on the variable parameters of process time, standoff distance, and shot mass flow rate. ANOVA indicated that the shot mass flow rate had the greatest impact on the roughness parameters ($p < 0.0001$). The roughness values of Ra, Rp, and Rv decreased as the shot's mass flow rate increased, and this decrease was more pronounced as the standoff distance diminished. The surface morphologies of the samples were notably modified by plastic deformation resulting from the repeated impact of shots. The water jet shot peening method modified the grains within the microstructure near the surface region. The grains in the microstructure were oriented perpendicularly to the peening direction to a depth of 5.36 μm beneath the surface, even at minimal peening levels. The surface hardness increased by approximately 64% relative to the hardness of untreated Ti6Al4V alloy (512.43 Hv versus 311.52 Hv), attributed to significant plastic deformation and strain hardening induced by the high kinetic energy of the impacting shots during water jet peening.

1. Introduction

Titanium alloys possess superior properties, including high strength, biocompatibility, and corrosion resistance, making them suitable for a wide range of applications in various industries. However, the growing demand for industrial applications and technological advancements requires the enhancement of surface and subsurface properties of titanium alloys, such as wear resistance and hardness [1]. In certain applications, such as artificial hip joints [2, 3], artificial knee joints [4], total hip arthroplasty [5], bone plates [6], spinal fusion implants [7], dental implants [8], and orthopaedic screws [9], the surface properties of titanium alloys are of paramount importance. Consequently, a proper implementation of surface treatment strategies is crucial for tailoring both surface and subsurface characteristics of titanium alloys; covering surface and subsurface hardness, microstructural characteristics, morphology, topography, tribological, corrosion, and biological properties [3, 10–12].

Numerous mechanical surface treatment techniques, including sandblasting (grit blasting) [13], laser texturing (peening), [14, 15] and shot peening [15–17] are often preferred due to their ease of application, cost-effectiveness, and time efficiency [1]. Among them, shot peening is the predominant technique over the past two decades for enhancing the surface properties of various alloys [18]. Conventional shot peening is an efficient, straightforward, and cost-effective technique [16, 17]; however, shot peening process mostly results in a rougher surface finish and may cause the embedding of shots into the target surface [19, 20]. Ultrasonic shot peening (USP), a more recent technique compared to conventional shot peening, can improve the deterioration of surface roughness caused by shot peening [21, 22]; however, it is not suitable for large-scale applications due to higher equipment costs and more complex procedures [23]. A significant constraint of laser peening is its thermal effect, especially when treating materials with a low melting point [19]; furthermore, the equipment cost is a concern [23]. These methods are also largely inapplicable to materials with high mechanical properties, such as hard metals and superalloys, due to insufficient peening pressure and intensity. Furthermore, the duration of peening markedly rises to attain high deformation rates for high-strength materials, including titanium alloys and superalloys [18]. As previously emphasized, the embedding of shots causes the contamination of the treated surface of materials, which may become highly problematic for biomedical applications.

Due to the aforementioned potential drawbacks, novel peening techniques are being explored for the surface modification of materials, especially for titanium alloys. To mitigate these drawbacks, recent advancements have introduced peening techniques utilizing water as the jet medium, including cavitation peening (CP) [24], wet shot peening [25], water jet peening (WJP) [26] (continuous water jet (CWJ), pulsating water jet (PWJ), ultrasonic pulsed water jet (UPWJ) peening [19, 27]), and abrasive water jet (AWJ) [19, 20, 28]. CP utilizes the impact generated by the collapse of cavitation bubbles for peening operations that can be applied to workpieces with complex shapes and does not require a very high injection pressure pump [24]. AWJ involves the impact of a high-velocity waterjet containing abrasive particles upon the surface of the material [12, 19]. In AWJ, sparsely embedded abrasive particles throughout the generated surface may cause contamination [29]. AWJ may also notably increase the surface roughness, which can lead to a poor appearance and fatigue crack initiation [12] and induce surface erosion under certain processing parameters [30]. To overcome the limitations in AWJ, researchers are considering WJP (CWJ and PWJ) [19] as an alternative surface enhancement technique due to its minimal corner constraints, simplicity of operation, low cost, high flexibility and geometrical accessibility, and environmental friendliness [23, 26]. Specifically, PWJ can be applied without adding solid particles (i.e., abrasive-less) and can be employed in the treatment of structural components for medical applications [27]. Although these technologies offer previously mentioned advantages, they also contain disadvantages such as the technological complexity of the fabrication of self-acting fluid oscillators or wear of the mechanical parts of the rotating disc [20], and elevated supply pressure is required for surface treatment [19, 29]. Finally, although WJP techniques can enhance surface residual stresses and surface and subsurface hardness, they may also induce surface erosion depending on the processing parameters [28].

A hybrid process that combines AWJ machining and shot peening has very recently emerged. The main principle of water jet shot peening involves introducing shots into a high-pressure water jet. Shots and/or abrasives are directed at the surface of the target material for modifying the surface and mechanical properties [31, 32]. AWJ machining, combining hard abrasives such as garnet and high-pressure water in a mixing chamber, uses a jet generated by a nozzle to direct the flow towards the workpiece [33, 34]. The shot peening involves repeated peening exposure of the target material with the aid of a nozzle of shot media, which is added to compressed air instead of water [17, 35]. Water jet shot peening represents a novel hybrid approach that aims to integrate the benefits of AWJ and shot peening techniques. The utilisation of water jet shot peening on materials results in energy levels notably higher than those achieved through conventional peening techniques while also substantially decreasing processing times. Furthermore, the movement of the shots within the jet reduces the probability of scattering and embedding within the target material. This results in a lower level of contamination on the surface, which is desirable for the biomedical field. The active presence of shots in the peening process is distinguished by the plastic deformation capability of the target material. An increased peening intensity per unit area could lead to disparate processing mechanisms such as cutting and wear.

A thorough review of the literature indicates that the significance of this hybrid innovative method has become apparent in recent years. Figure 1(a) illustrates that research on the utilisation of water jet peening has notably increased in the last three years, while the method has been mostly applied on titanium alloys (figure 1(c)). Alumina and steel shots were the predominant materials utilized in water jet shot peening as the peening media (figure 1(b)). Water jet shot peening has the potential to enhance surface and subsurface microstructural, morphological, and mechanical characteristics, along with fatigue properties. Research is needed to elucidate the influences of water jet shot peening on the surface and sub-surface properties, including surface roughness, morphology, topography, hardness, and microstructure.

Ti6Al4V alloy, which is widely utilized in biomedical and aerospace applications, has been the subject of extensive investigation about its suitability for the water jet shot peening process (table 1). Alumina and

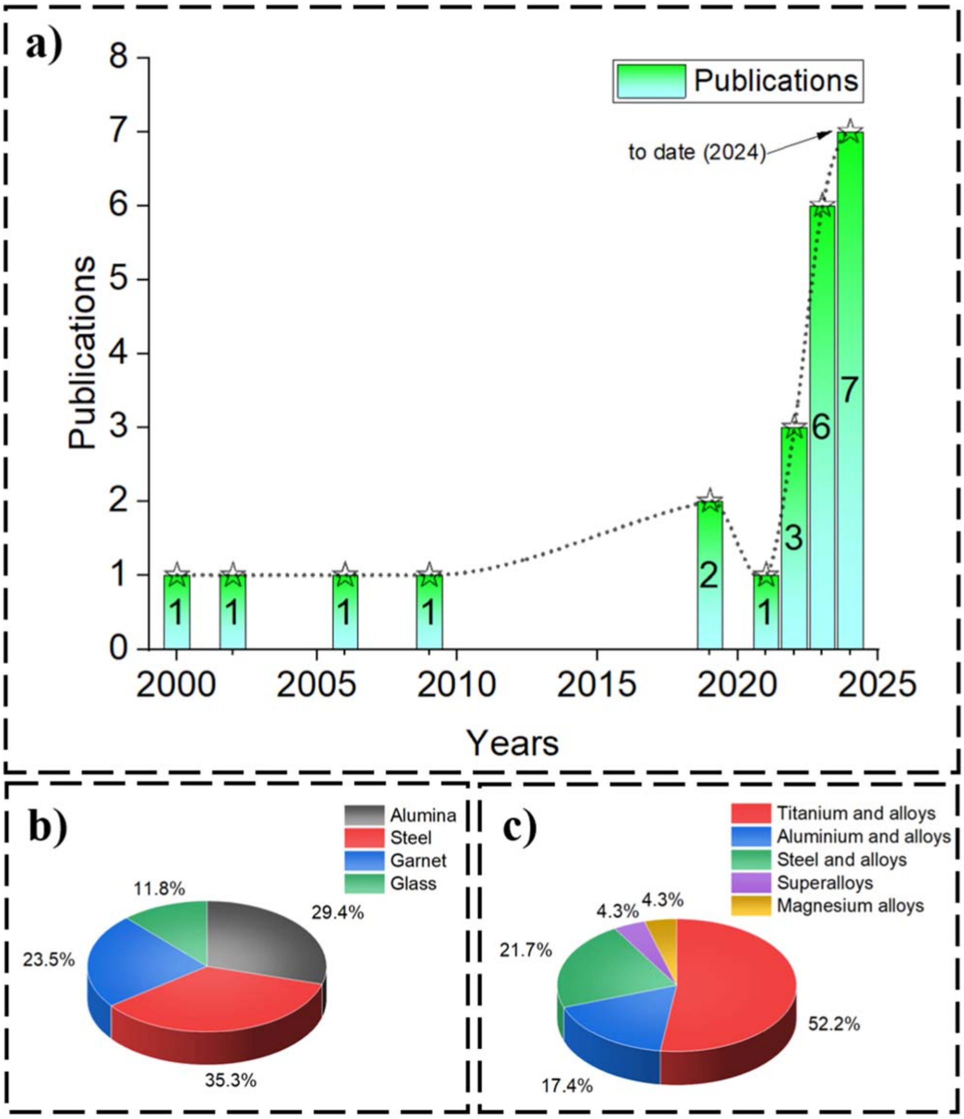

Figure 1. Publications on water jet shot peening in the literature: (a) year, (b) material, (c) abrasive (peening) material (According to a search in SCOPUS® database in August 2024).

stainless-steel shots are predominantly selected as peening materials, and pressure is often included in the studies as a key parameter. Overall, the process parameters play a crucial role in the ultimate properties of the peened titanium alloy. Regarding AWJ, traverse speed, abrasive mass flow rate, and standoff distance are the principal parameters influencing machining performance. In the peening process, the total kinetic energy of the shots acting on a unit area in unit time is determined by these parameters. Consequently, a limited number of studies have investigated these parameters (table 1) addressing the application of water jet shot peening with stainless steel shots for modifying the surface and subsurface properties of Ti6Al4V alloy. Further research into the correlation between key processing parameters (i.e., process duration, standoff distance, and shot mass flow rate) and the resultant surface morphology, topography, roughness, as well as surface and subsurface microstructure and hardness is required. The current study aims to address this gap by employing water jet shot peening on cold-rolled Ti6Al4V sheets under various processing parameters, elucidating the correlation between the modified properties of the alloy (surface, subsurface, and mechanical properties) and the parameters of the water jet shot peening process.

The present study investigates the surface and subsurface characteristics of cold-rolled Ti6Al4V sheets subjected to water jet shot peening, with the objective of elucidating the effects of peening parameters on these properties. The effects of process time, standoff distance, shot mass flow rate parameter, and parameter levels on surface roughness were examined using ANOVA. The optimal parameter values were identified based on the equal significance attributed to the surface roughness parameters (Ra, Rp, and Rv). Investigation criteria were optimal and suboptimal solution parameter levels of surface roughness, surface and subsurface morphological, and microstructural characteristics. Selected samples were subsequently analysed using stereo microscopy and

Table 1. Summary of research on water jet shot peening on titanium alloys [32, 36–43].

Year (references)	Target material	Peening media	Variable parameters	Primary outcome
2023 [36]	Ti6Al4V	304 stainless steel	—	Improved hardness and erosion resistance
2022 [37]	TC4 titanium alloy	304 stainless steel	Pressure, standoff distance, traverse speed	Increased surface roughness, improved hardness and residual stress development
2019 [39]	Ti6Al4V	Alumina	Pressure, pre-stress, abrasive mesh size	Obtained compressive residual stress
2022 [38]	Ti6Al4V	—	—	Prolonged fatigue life
2019 [40]	Ti6Al4V	Alumina	—	Increased fatigue strength
2002 [41]	Ti6Al4V and Cp-Ti	Garnet	Pressure, abrasive mesh size	Increased surface roughness and compressive residual stress
2023 [32]	Ti6Al4V	Alumina	—	Enhanced corrosion resistance
2023 [42]	TA19 alloys	304 stainless steel	Pressure, standoff distance	Increased surface roughness and fatigue life
2006 [44]	Ti6Al4V	Garnet	Pressure, standoff distance, traverse speed, abrasive mesh size	Residual stress and fatigue life increase
2000 [43]	Ti6Al4V	Garnet	Pressure, abrasive mesh size	Prolonged fatigue life

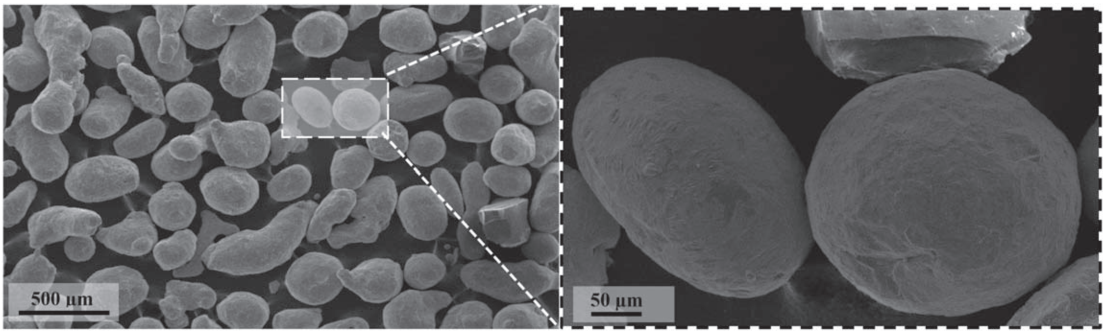

Figure 2. SEM images of the stainless-steel shots used for water jet shot peening of titanium alloy samples.

Table 2. Chemical, mechanical, and physical properties of Ti6Al4V [16].

Ti6Al4V	Grade 5 (R56400)
Chemical composition (% wt)	C: 0.8, Fe: 0.25, N: 0.05, O: 0.2, Al: 5.50–6.75, V: 3.5–4.5, H: 0.015
Ultimate strength	896 MPa
Yield strength	827 MPa
Nominal hardness	33 HRC
Density	4.43 g cm^{-3}
Melting point (approximate)	1,650 °C

scanning electron microscopy. Subsequent microhardness measurements revealed changes in surface and subsurface hardness.

2. Materials and methods

2.1. Materials

Ti6Al4V Grade 5 was obtained from TIMET (Titanium & Medical & Mining Company, Turkiye) in the form of cold-rolled sheet. The specimens were formed by guillotine shear cutting with a thickness of 1.5 mm and dimensions of 20 × 50 mm. Table 2 presents the chemical, mechanical, and physical properties of titanium alloy. Stainless steel shots with a diameter of between 0.1 and 0.3 millimetres were utilised in the water jet shot peening process (figure 2).

2.2. Water jet shot peening of samples

Figure 3 illustrates the water jet shot peening process. In the water jet stage, high-pressure water passes through an orifice, and the steel shots enter the mixing chamber at a predetermined flow rate through a metering unit. The combination of high-pressure water and shots creates a jet flow with the nozzle, resulting in a bombardment of the target material. In the shot peening stage, balls with high kinetic energy create plastic deformation on the surface of the material through repeated impact. Furthermore, the application of cold forming results in the generation of residual compressive stresses and an increase in hardness beneath the surface.

The water jet shot peening process (figure 4) was conducted on a 3-axis CT brand AWJ machine, equipped with a 50 HP pump (KMT brand). The processing parameters have been established using manufacturer recommendations for AWJ machines, in line with literature (table 1) and authors' process experience [32, 36–43], and can be found in table 3. The experimental design employed in the present study is a full factorial design, with the objective of obtaining the machining performance results according to all conditions of the parameter levels that were experimentally investigated. This approach was adopted to minimise the potential for errors in the results arising from the effects of the experimental parameters and their interactions, as evidenced by ANOVA. Accordingly, an L18 full factorial experimental design was employed to ascertain the influence of the parameters on the surface roughness, with the results analysed using ANOVA. The analyses were conducted using Design-Expert 13 software, and the optimal parameters were identified based on the surface roughness parameters.

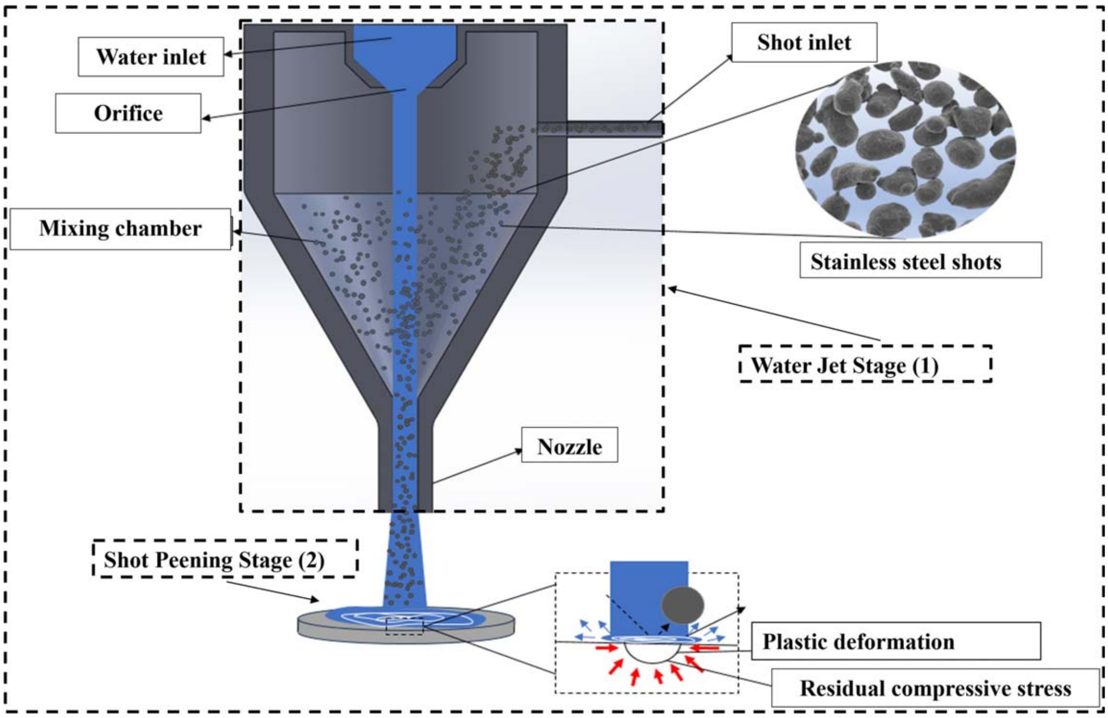

Figure 3. Representation of the water jet shot peening process of titanium alloy samples.

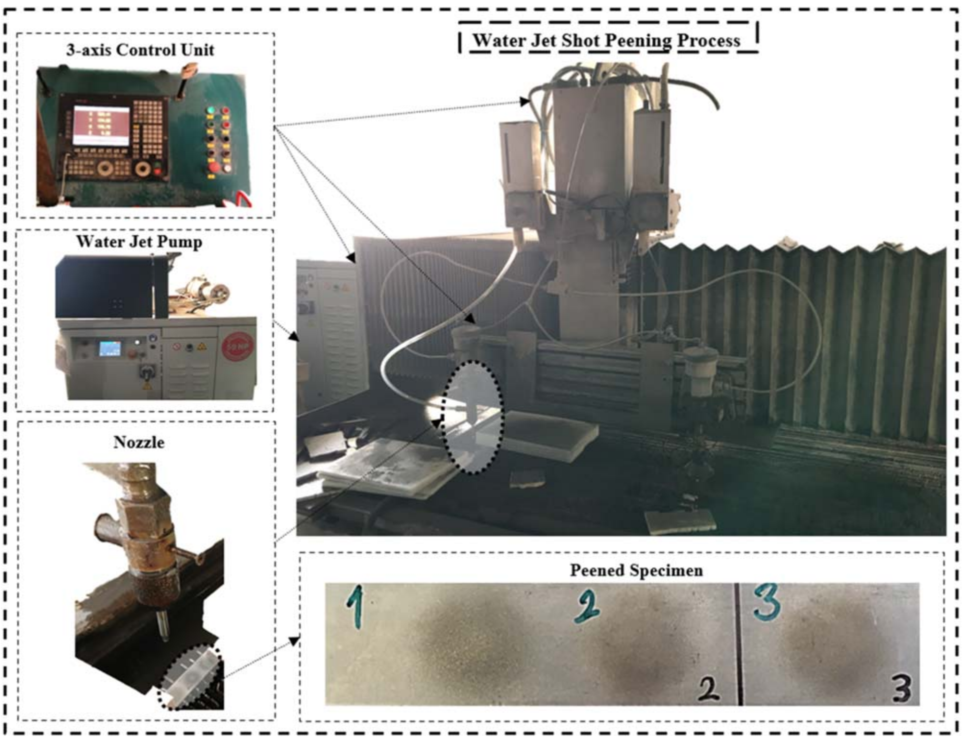

Figure 4. Water jet shot peening process and peened specimen.

2.3. Specimen preparation for surface and subsurface investigations

To investigate the effects of water jet shot peening on the surface properties, the peened samples were cleaned with alcohol in an ultrasonic bath. For examining subsurface properties, specimens were prepared through precision cutting of peened samples. This comprised a cross-section through the circular region's centre, where water jet shot peening was implemented. Following the cutting process, the specimens were metallographically prepared through grinding using SiC grinding papers (320–2000 mesh), polishing with 6 μm, 3 μm, diamond

Table 3. Processing parameters of water jet shot peening.

Parameters	Value(s)	Units
Shot mass flow rate	14, 20	g/s
Peening time	3, 5, 7	s
Standoff distance	70, 80, 90	mm
Pressure	170	MPa
Nozzle diameter	0.76	mm
Orifice diameter	0.25	mm
Nozzle impact angle	90	°(degree)
Shot dimensions	0.1–0.3	mm

solution, and 1 μm and colloidal silica. Finally, the specimens were etched using a Kroll solution (1 ml HF, 3 ml HNO_3, and 96 ml distilled water). Then, subsurface features were imaged using an optical microscope at 10 × and 50 × magnification. Furthermore, for more detailed examinations, secondary electron scanning electron microscope (SEM) images were captured with a gaseous secondary electron detector (GSED) at 1000 × to 50000 × zoom ratios using a scanning electron microscope (ESEM-thermoscientific Quattro S) with an Everhart-Thornley detector (ETD).

2.4. Characterisation of surface roughness

The average surface roughness (Ra) was selected as the parameter to be analysed in the present study, as it is the most commonly studied surface roughness parameter in the literature. However, in order to determine the absolute effect of water jet shot peening on surface roughness, the machining procedure was applied pointwise. Consequently, the resulting surface roughness performances were evaluated in terms of surface roughness parameters, including average (Ra), maximum peak depth (Rp), and maximum valley depth (Rv) roughness. Surface roughness measurement was carried out with a Mitutoyo brand (SJ-301 model) contact-type stylus profilometer. The measurement parameters were as follows: cut-off wavelengths of 2.5 mm/8 μm, an evaluation distance of 12.5 mm, and a Gaussian filter. Each measurement was repeated five times and averaged. In addition, a full factorial experimental design was employed in order to minimise variability and repeatability errors by accounting for parameter level changes in the data. The data were validated using the statistical p-value result of the ANOVA model obtained.

2.5. Characterisation of surface morphologies and topographies, subsurface morphologies, and mechanical properties

The surfaces processed with water jet shot peening were initially examined using an optical microscope at 5 × and 10 × magnification. Subsequently, optical profilometer (Huvitz brand) scans were conducted at zoom ratios spanning from 5 × to 50 × . Finally, secondary electron images were obtained using the SEM described in the previous sub-section.

The subsurface microhardness of the alloy processed by water jet shot peening was quantified from prepared cross-sectional specimens. Vickers microhardness measurements (Zwick brand) were conducted in accordance with the ASTM E348-17 standard. Measurements were conducted at 20 μm intervals from the surface to a depth of approximately 350 μm, with a dwell time of 10 s and a load of 0.2 kg. Then, the variation in hardness as a function of depth was assessed.

3. Results and discussion

Table 4 illustrates the L18 full factorial experimental design and the resulting surface roughness values. The application of the experimental design enabled the performance of ANOVA analyses, which yielded the optimal levels of the experimental parameters in accordance with the results.

The results of the analysis of variance (ANOVA) for the Rp, Rv, and Ra parameters are presented in table 4. The fit for models were statistically significant (i.e., $p < 0.05$). The R-squared values (0.9154, 0.8145, and 0.9262, respectively) were satisfactory as the difference between the adjusted R-squared values was less than 0.2. The signal-to-noise ratio (Adeq Precision) measurements of the models exceed 4, corroborating the veracity of the findings. The results demonstrate that the most influencing experimental parameter is the shot mass flow rate (statistically significant). The parameter interactions were negligible, which could be interpreted as the absence of a threshold value that would alter the behavioural trends of the two parameter levels.

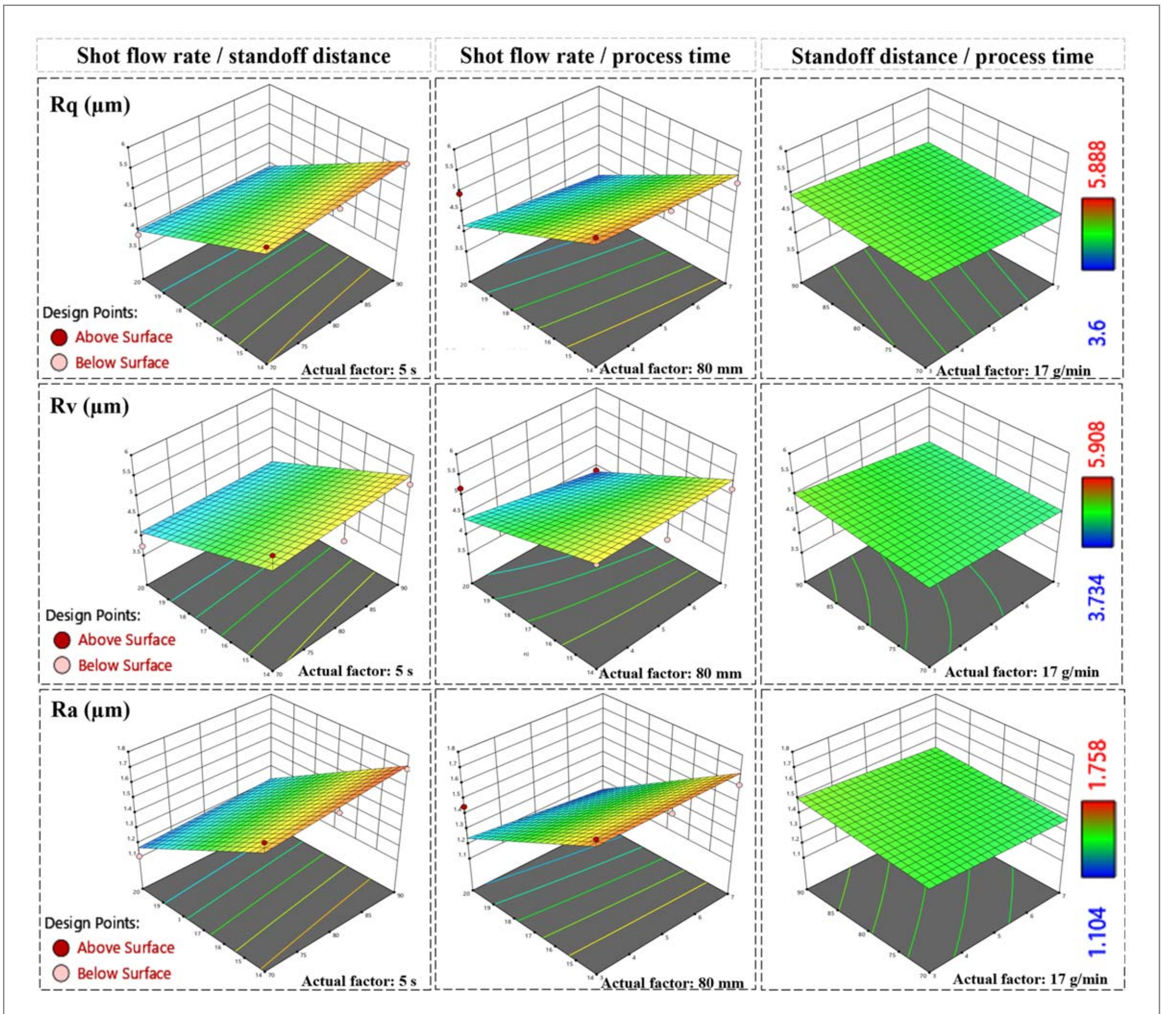

Figure 5. Surface roughness (Rp, Rv, Ra) behaviour at parameter and parameter levels.

Table 4. L18 full factorial experimental design and resultant roughness values.

Test no	Process time (s)	Standoff distance (mm)	Shot mass flow rate (g/min)	Rp (μm)	Rv (μm)	Ra (μm)
1	3	70	14	5.32	5.05	1.59
2	3	70	20	3.99	4.36	1.18
3	3	80	14	5.83	5.36	1.74
4	3	80	20	4.96	5.19	1.45
5	3	90	14	5.89	5.91	1.76
6	3	90	20	3.72	4.15	1.17
7	5	70	14	5.58	5.61	1.71
8	5	70	20	3.87	3.74	1.11
9	5	80	14	5.49	4.90	1.66
10	5	80	20	3.83	3.73	1.10
11	5	90	14	5.66	5.31	1.71
12	5	90	20	3.82	4.07	1.19
13	7	70	14	5.42	5.48	1.69
14	7	70	20	3.83	4.06	1.16
15	7	80	14	5.26	5.17	1.62
16	7	80	20	3.60	3.87	1.12
17	7	90	14	5.67	5.70	1.76
18	7	90	20	3.95	4.01	1.22
			St. Dev.:	0.8873	0.7483	0.2725
			CI (95%):	4.351–5.170	4.414–5.105	1.315–1.567

Figure 5 illustrates the surface roughness behaviours of the experiments conducted in accordance with sets of parameters (i.e., different values for a specific parameter where other parameters kept constant) outlined in table 4. As the shot mass flow rate increased, the roughness values (Ra, Rp, Rv) decreased, also proportional to

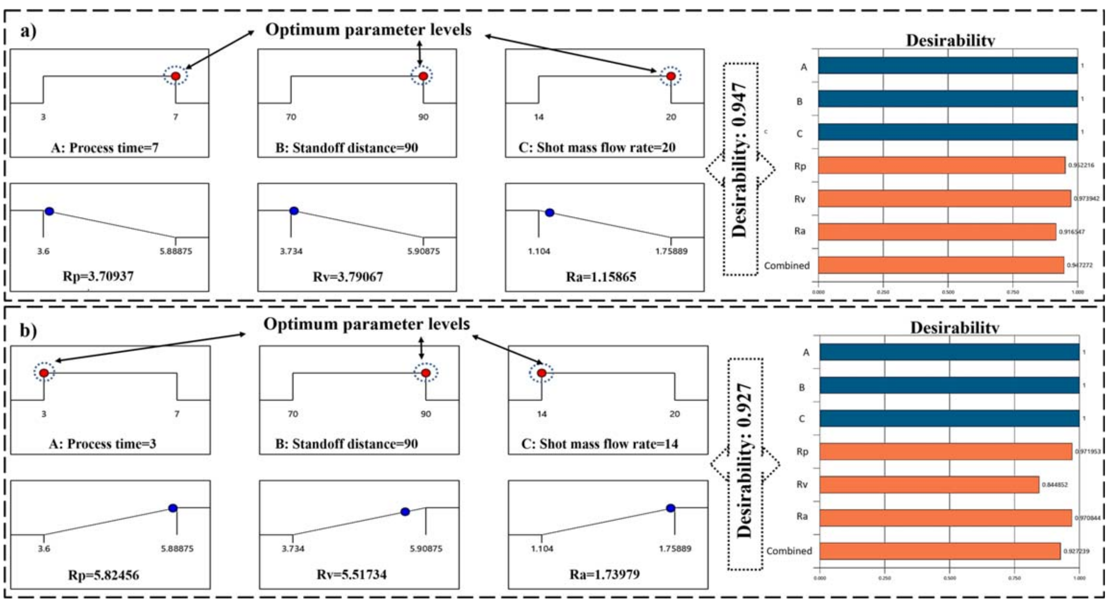

Figure 6. Combined optimisation with Rp, Rv, and Ra: (a) minimum solution, (b) maximum solution.

declines in standoff distance. Similarly, the roughness values decreased further as the shot mass flow rate and process time increased. The surface roughness varied at the same shot mass flow rates, similarly, standoff distance and process time also varied. Nevertheless, the graph produced based on the sets of parameter sets did not exhibit a distinctive behaviour, which could be attributed to limited effects of parameters and insignificant interactions. Zhang *et al* [31] applied water jet peening to 7075-T6 aluminium alloy and reported that the surface roughness decreased with increasing transverse speed due to a change in the area covered per unit time. It should be noted that a similar decrease was observed under conditions where the standoff distance increased.

The determination of sets of parameter for the target surface performance is of utmost importance in the context of industrial applications and contributions. Consequently, the results of the optimisation of Rp, Rv, Ra are presented in figures 6(a) and (b). Concerning the maximum and minimum solutions, it can be stated that the process time and shot mass flow rate parameter sets exhibit a similar approach, while the standoff parameter value is maintained. This situation can be tested with the interaction results presented in table 5. The combined desirability results (demonstrating the precision of optimisation outcomes) were 0.947 and 0.927 for the minimum and maximum solutions, respectively. This approach enabled the establishment of design conditions for researchers and practitioners and the provision of relationships for other characterisation results of the study. Since the shot mass flow rate is the key experimental parameter in this study, the subsequent section will conduct morphological and topographical analyses to clarify the underlying reasons for the observed performance of the parameters and their levels.

3.1. Effects of process parameters on surface morphology and topography

The optimisation of surface roughness data indicates that it is beneficial to examine surface topography while varying process duration and shot mass flow rate, with standoff held at its optimal value. Figure 7 presents comparative 2D and 3D surface topographies showing the effects of changing parameter levels. The surface topographies demonstrate the dominant effect of shot mass flow rate (the most influential parameter per table 5). The dimensions of crater structures, which are composed of peaks and pits on the surfaces, are reduced because of an increase in the amount of shot mass flow rate, specifically to 20 g min^{-1}. This indicates that with an increase in the amount of shot impacting per unit area, plastic deformation forms more uniform surface topography. The size of the crater structures increased as the process time was reduced because of a decrease in the number of shots that impacted the unit area.

Figure 8 provides SEM images of the peened surfaces under different water jet shot peening parameters. It was observed that the Ti6Al4V surface was formed into crater structures, which included pits and peaks, as a result of high-pressure water and high kinetic energy shots. Additionally, the dimensions of the craters are linked to changes in sets of parameters and process parameters. It was observed that the plastic deformation is

Table 5. ANOVA results for Rp, Rv, and Ra.

Source	Sum of squares	df	Mean square	F-value	p-value	
Rp						
Model	12.26	6	2.04	19.83	<0.0001	significant
A- Process Time	0.3303	1	0.3303	3.21	0.1009	
B-Standoff distance	0.0392	1	0.0392	0.3802	0.55	
C-Shot mass flow rate	11.75	1	11.75	114.08	<0.0001	
AB	0.0007	1	0.0007	0.0068	0.9358	
AC	0.0297	1	0.0297	0.2884	0.602	
BC	0.1037	1	0.1037	1.01	0.3373	
Residual	1.13	11	0.103			
Cor Total	13.39	17				
Rv						
Model	7.73	6	1.29	8.05	0.0016	significant
A-Process Time	0.2467	1	0.2467	1.54	0.2402	
B-Standoff distance	0.0595	1	0.0595	0.372	0.5543	
C-Shot mass flow rate	7.09	1	7.09	44.28	<0.0001	
AB	0.0289	1	0.0289	0.1804	0.6792	
AC	0.267	1	0.267	1.67	0.223	
BC	0.0424	1	0.0424	0.2646	0.6171	
Residual	1.76	11	0.16			
Cor Total	9.49	17				
Ra						
Source	Sum of Squares	df	Mean Square	F-value	p-value	
Model	1,16	6	0,1936	23	<0.0001	significant
A- Process Time	0,009	1	0,009	1,07	0,3235	
B-Standoff distance	0,0118	1	0,0118	1,4	0,261	
C-Shot mass flow rate	1,13	1	1,13	134,62	<0.0001	
AB	0,0001	1	0,0001	0,0128	0,9118	
AC	0,0066	1	0,0066	0,788	0,3937	
BC	0,0009	1	0,0009	0,1054	0,7516	
Residual	0,0926	11	0,0084			
Cor Total	1,25	17				

Abbrevations: df: degrees of freedom; Rp: maximum peak depth roughness; Rv: maximum valley depth roughness; Ra: average surface roughness; AB, AC, BC: relevant binary parameter interaction

unaffected by the standoff distance, whereas a substantial improvement was observed as a result of an increase in the shot mass flow rate. It is possible to assert that the size of the crater structures on the surface slightly increases as the standoff distance decreases. Finally, none of the surface morphologies exhibited any undesirable defect, including cracks.

Figure 9 depicts the potential micro-processing mechanisms that may occur within the context of high-magnification SEM images captured from the peened surfaces (figure 9(a): micro adhesion wear, 9-b: micro abrasive wear at the crater boundaries, 9-c: the reduction in crater size resulting from a decrease in the standoff distance parameter in comparison to 9-a and -b, 9-d: impact of an elevated shot mass flow rate parameter on the reduction in crater size formation). Additionally, micro adhesion and micro shear formation were observed. Consequently, the formation of micro-adhesion, micro-cutting, and micro-abrasive wear was observed under the influence of significant plastic deformation.

3.2. Effects of process parameters on subsurface microstructure

Figure 10 illustrates the alteration in subsurface microstructure in response to varying parameter levels. The water jet shot peening process resulted in the transformation of the homogeneous distribution of grains within the distinctive structures of the unprocessed cold-rolled material, creating a new orientation of grains close to the surface region. The increase in grain orientation depth was achieved by extending the process time and reducing the standoff distance, which was attributed to the increase in the amount of shot [45] and kinetic energy of the jet acting per unit area per unit time. Similarly, the standoff distance [46, 47] results in an increase in the quantity of shot and a hydrodynamic enhancement with the proximity to the effective jet area increasing. As a result, the plastic deformation effect arising from the variation of both parameter levels has formed the distance and development of grain orientation along the subsurface depth of the material. Yao *et al* [48] addressed the

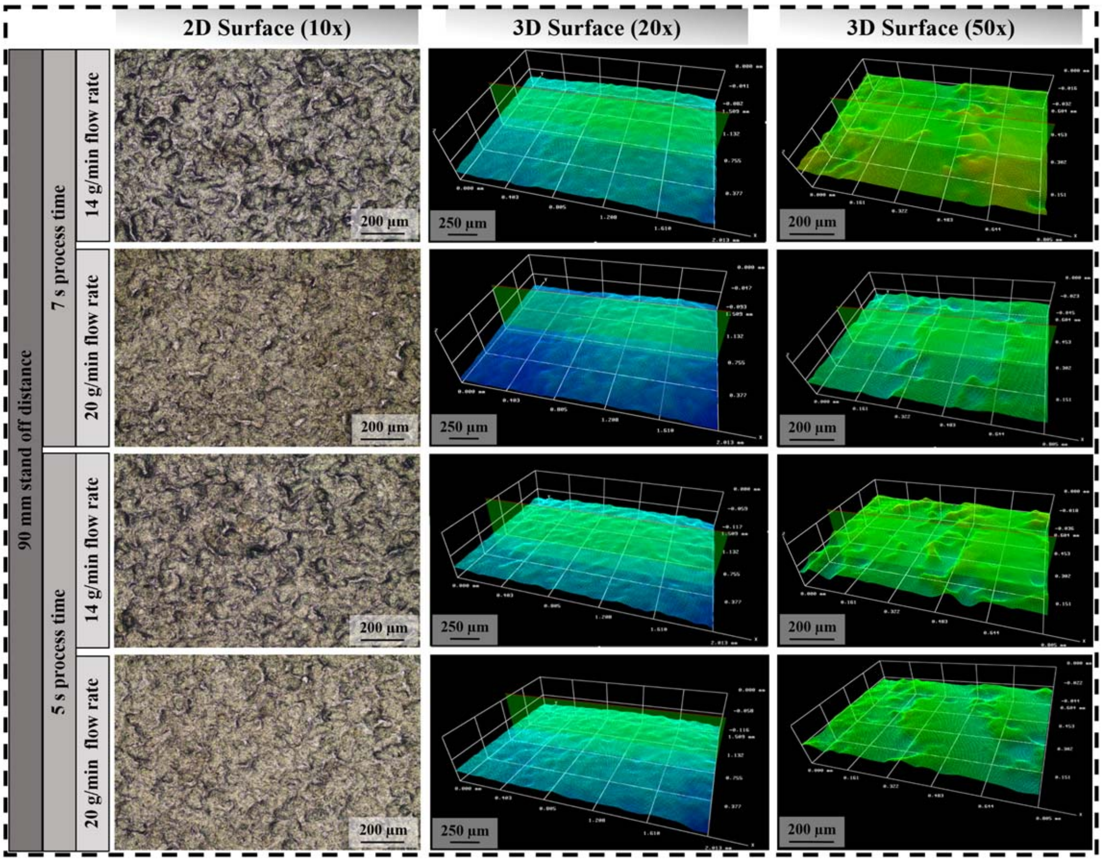

Figure 7. 2D (optical) and 3D (profilometer) surface topography for different parameter levels.

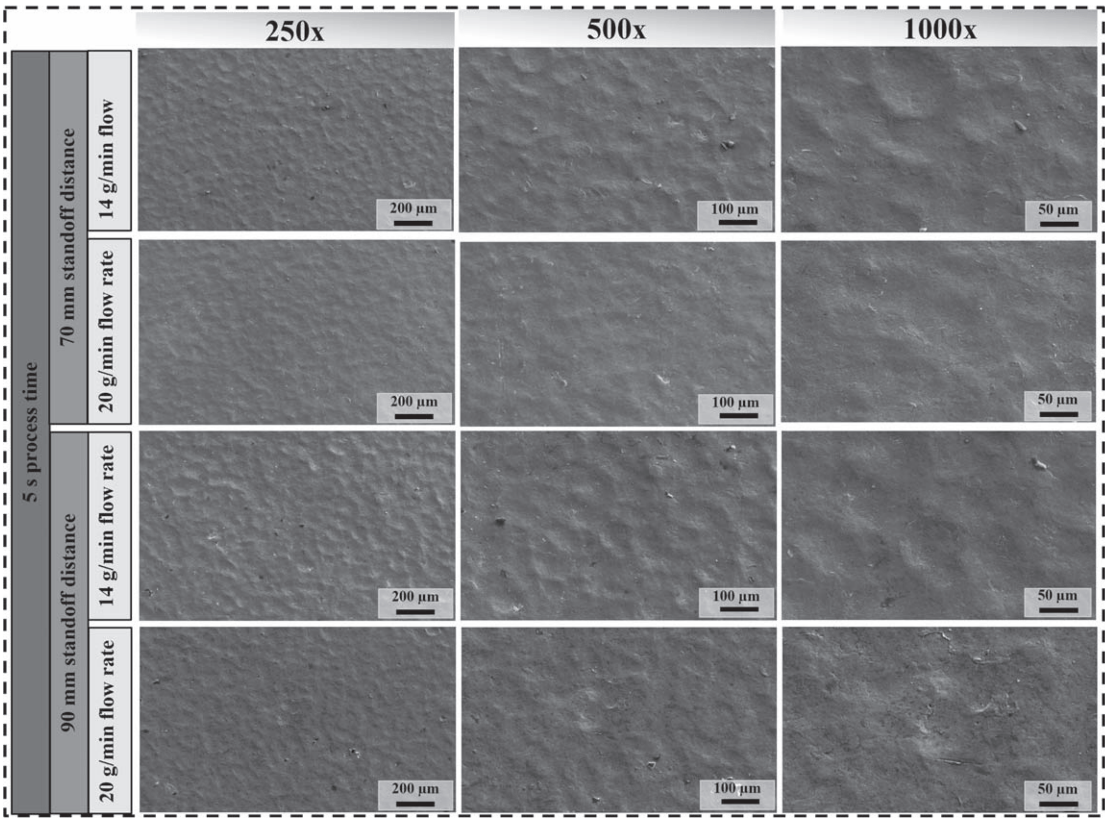

Figure 8. Surface morphology of peened samples under different parameters.

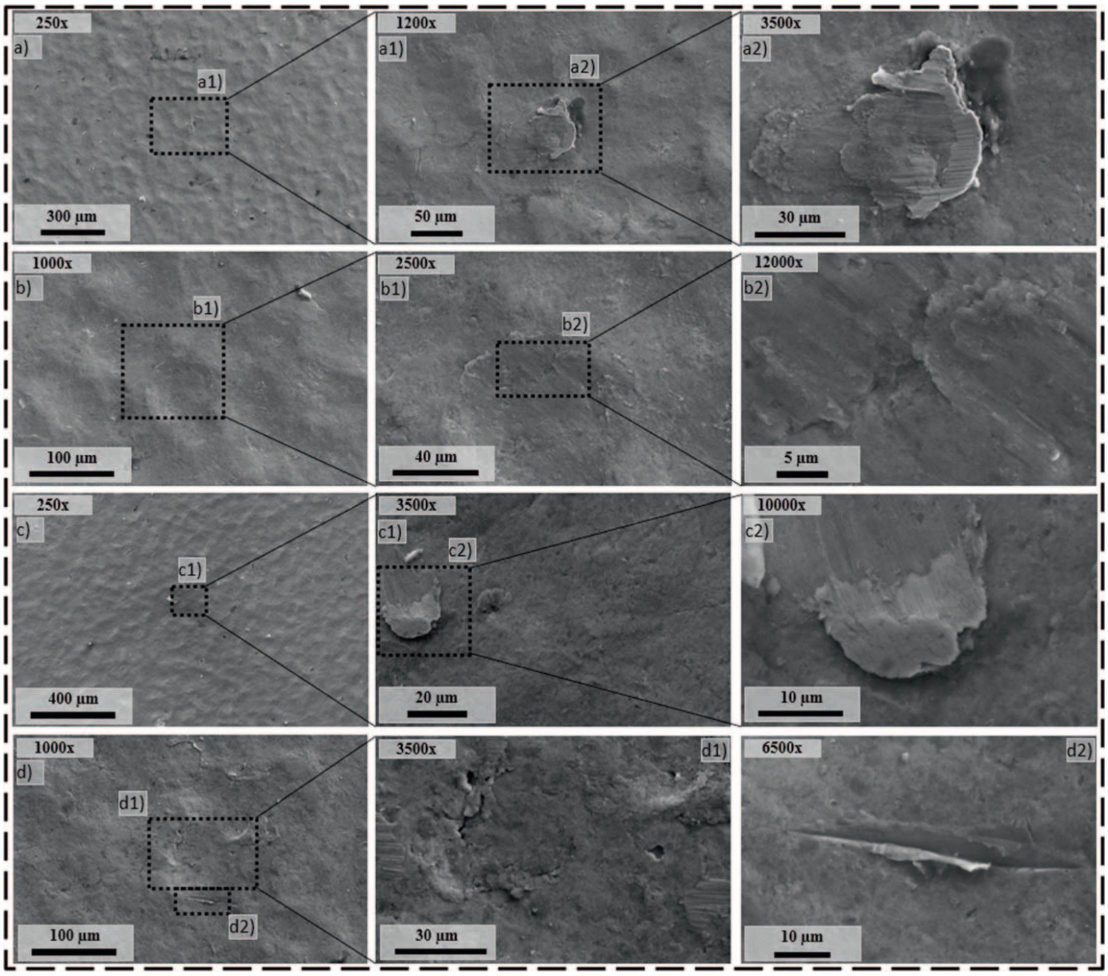

Figure 9. Micro-processing mechanisms: (a), (b) 5 s process time, 90 mm standoff distance and 14 g min^{-1} shot mass flow rate; (c) 5 s process time, 80 mm standoff distance and 14 g min^{-1} shot mass flow rate; 5 s process time, 90 mm standoff distance and 20 g min^{-1} shot mass flow rate.

variation in the depth of plastic deformation of nickel-based superalloys GH4169 under the influence of kinetic energy varying according to different processing parameter levels, revealing that the processing parameters have an influence on the resultant microstructural features.

3.3. Effects of process parameters on subsurface micro hardness

The effects of standoff distance and shot mass flow rate on surface and subsurface microhardness development under the maximum process time conditions are illustrated in figure 11. Hardness curves were produced using a fourth-order polynomial, which addresses hardness data in relation to depth. The alloy exhibited a notable increase in surface hardness, with an approximate 27–64% rise in accordance with the subsurface micro hardness averages under different processing parameters. The micro hardness values exhibited a rapid decrease as they penetrated deeper into the material, reaching a constant value at which the strain hardening effect was not observed. Nevertheless, despite the differences in parameter levels, the trend curves displayed a similar pattern. When the standoff distance was minimised and the shot mass flow rate was altered, the depth-dependent reduction in hardness was diminished, and the hardness retention was more pronounced under the surface. This is elucidated by the increase of the effective area of the jet, specifically the core region, which notably influences the kinetic energy of the projectiles per unit area. Moreover, the increased shot mass flow rate, which increases kinetic energy, improved the average hardness beneath the surface. In scenarios with a significant standoff distance and varying shot mass flow rate, the initial depth-dependent reduction was more pronounced. Nevertheless, an increase in the shot mass flow rate resulted in a notable enhancement in the average hardness.

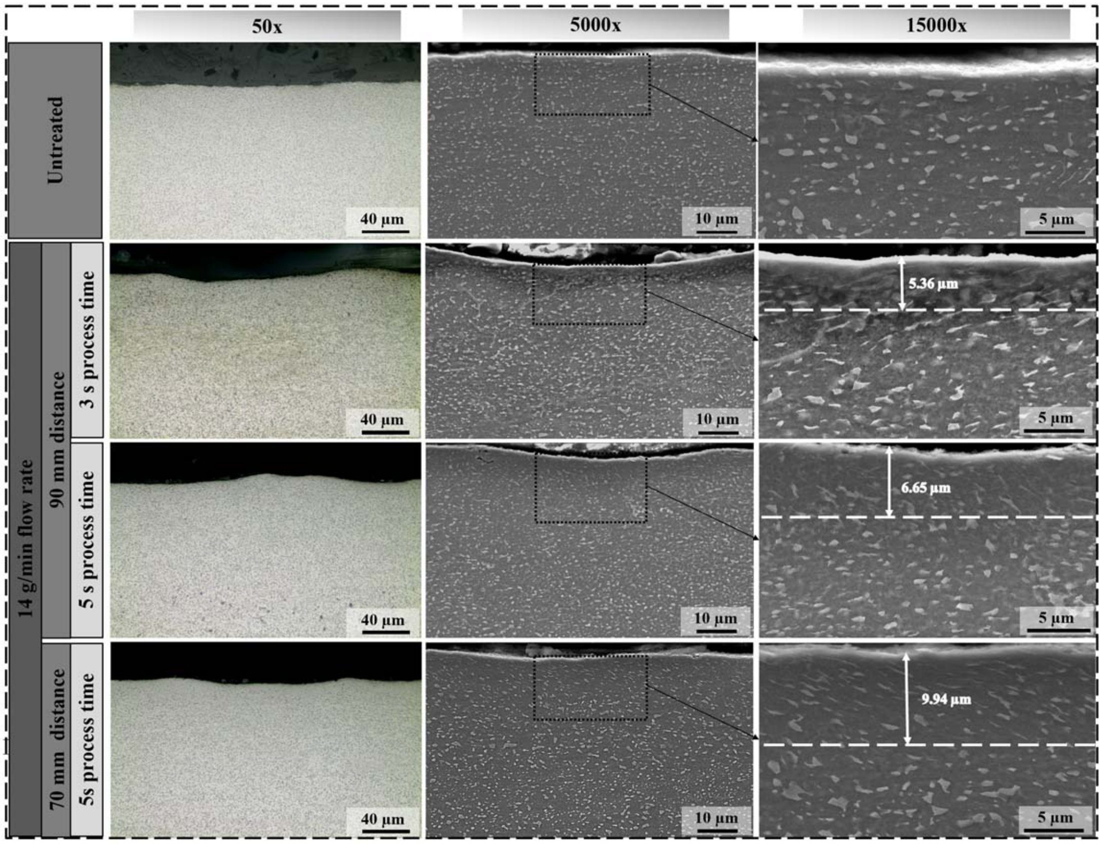

Figure 10. Subsurface microstructure behaviour by optical and scanning electron microscopy.

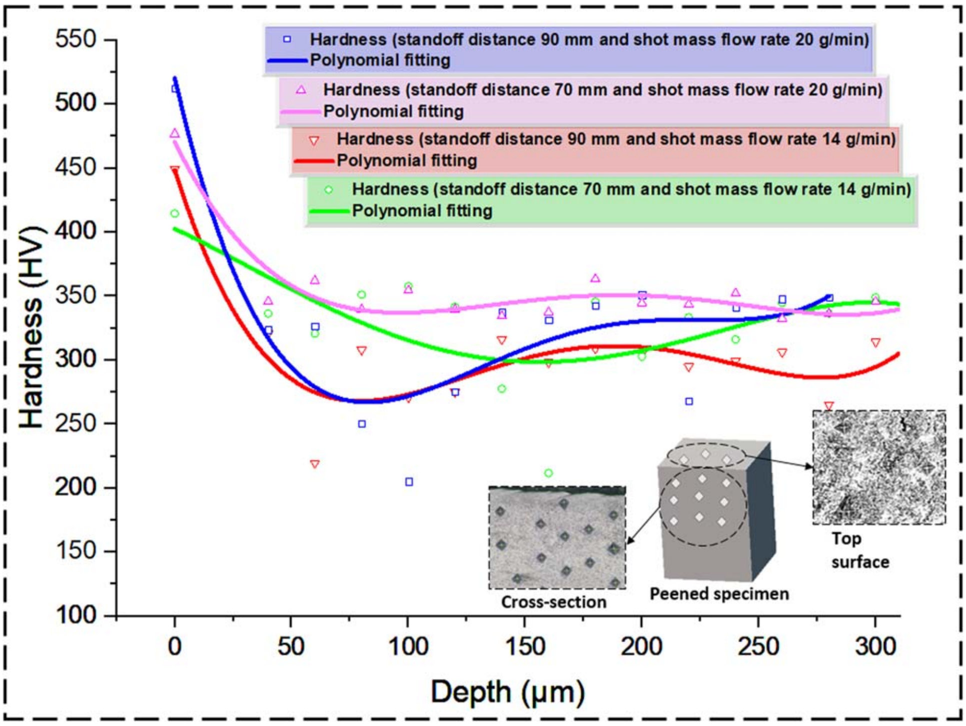

Figure 11. Surface and subsurface hardness behavior according to standoff distance and shot mass flow rate variation.

4. Conclusion

Water jet shot peening was applied on cold-rolled Ti6Al4V sheets following an L18 full factorial experimental design, focusing on the variable parameters of process time, standoff distance, and shot mass flow rate. Then, the modified surface and sub-surface properties of the alloy were examined under various processing parameters.

- The most influential experimental parameter for surface roughness was the shot mass flow rate, affecting kinetic energy by adjusting the number of shots per unit area per unit time. The roughness values of Ra, Rp, and Rv decreased as shot mass flow rate increased, and the decrease was more pronounced at lower standoff distances. The roughness values further decreased as the shot mass flow rate and process time increased.
- The high-pressure water and high kinetic energy shots that plastically formed the Ti6Al4V surface resulted in the formation of crater structures, which included pits and peaks. The dimensions of the craters are linked to changes in parameter levels and process parameters. The plastic deformation is unaffected by the standoff distance, whereas a substantial improvement was observed because of an increase in the shot mass flow rate. Surface morphologies did not exhibit any undesirable defects, including cracks.
- The orientation of grains near the surface was observed in all samples, even at low shot mass flow rates. In all cases, the minimum depth of grain orientation was limited to 5.36 μm. As the process time increased, the depth of grain orientation increased as well (e.g., 6.65 μm). Similarly, as the standoff distance decreased, the depth of grain orientation also decreased (e.g., 9.94 μm).
- The shot mass flow rate parameter demonstrated efficacy in maintaining the subsurface average hardness. The surface hardness exhibited an improvement of approximately 64% relative to the subsurface average hardness.

The findings contribute to the utilization of water jet shot peening to modify the surface and subsurface properties of titanium alloys, which are particularly useful in biomedical applications. The results will facilitate future research to address gaps in the current literature regarding the correlation between the modified properties of water jet peened alloys (surface, subsurface, and mechanical properties) and the parameters of the applied water jet shot peening process. The present study was able to establish optimal processing parameters using practical parameters for AWJ machines, in line with literature and authors' process experience. Future research should prioritize the examination of the effects of mesh parameters and mesh types, potential contamination and its long-term effects (which are the limitations of the current study), the application of alternative experimental design methodologies (e.g., Taguchi), and machine learning techniques (including artificial neural networks).

Data availability statement

The data presented in this article is derived from a scientific project that has not yet been completed. Consequently, we are unable to make all of the data available at this time until the project report has been submitted and published. The data that support the findings of this study are available upon reasonable request from the authors.

Funding

The authors acknowledge the financial support by Kocaeli University Scientific Research Projects Coordination Unit (Project Number: FCD-2023-3305).

ORCID iDs

Egemen Avcu https://orcid.org/0000-0002-3244-1316
Mustafa Armağan https://orcid.org/0000-0003-0429-0351

References

[1] Abakay E, Armağan M, Yıldıran Avcu Y, Guney M, Yousif B F and Avcu E 2024 Advances in improving tribological performance of titanium alloys and titanium matrix composites for biomedical applications: a critical review *Frontiers in Materials* **11** 1–32
[2] Ji R, Chen F, Ying R and Zhang L 2023 Ceramic-titanium alloy artificial hip joint wear simulation and experimental study *Coatings* **13** 1–18

[3] Klichova D, Nag A, Poloprudský J, Foldyna J, Pude F, Sitek L and Hloch S 2023 Utilising of water hammer effect for surface roughening of Ti6Al4V *Int. J. Adv. Manuf. Technol.* **126** 5633–47
[4] Ji R, Qi Z, Chen J, Zhang L, Lin K, Lu S and Li Y 2023 Numerical and experimental investigation on the abrasive flow machining of artificial knee joint surface *Crystals* **13** 1–12
[5] Wirries N, Becker R E and Skutek M 2024 Failure of total hip arthroplasty due to delamination and wear of titanium nitride-coated titanium heads: a case series *J. Orthop. Case. Rep.* **14** 36–9
[6] Wang G, Wang S, Yang X, Yu X, Wen D, Chang Z and Zhang M 2021 Fretting wear and mechanical properties of surface-nanostructural titanium alloy bone plate *Surf. Coat. Technol.* **405** 1–10
[7] Towers W S and Kurtom K 2020 Rare systemic response to titanium spinal fusion implant: case report *Cureus* **12** e7109
[8] Hossain N, Islam M A, Shakib Ahmed M M, Chowdhury M A, Mobarak M H, Rahman M M and Helal Hossain M D 2024 Advances and significances of titaniumin dental implant applications *Results in Chemistry* **7** 1–12
[9] Rotella G, Morano C, Saffioti M R and Umbrello D 2024 Surface functionalization of titanium screws for orthopaedic implant applications *CIRP Ann.* **73** 453–6
[10] Gao K, Zhang Y, Yi J, Dong F and Chen P 2024 Overview of surface modification techniques for titanium alloys in modern material science: a comprehensive analysis *Coatings* **14** 1–40
[11] Fu Y, Wang G, Gao J, Yao Q and Tong W 2020 New approach to produce a nanocrystalline layer on surface of a large size pure titanium plate *Coatings* **10** 1–10
[12] Chakkravarthy V, Manojkumar P, Jerome S, Evlashin S A, Arackal Narayanan J, Mendagaliev R V, Sidorenko A O and Narayan R L 2024 Effect of impact angle on hot corrosion resistance of abrasive water jet peened Ti-6Al-4V alloy *Surf. Coat. Technol.* **494** 1–10
[13] Avcu E, Yıldıran Avcu Y, Baştan F E, Rehman M A U, Üstel F and Boccaccini A R 2018 Tailoring the surface characteristics of electrophoretically deposited chitosan-based bioactive glass composite coatings on titanium implants via grit blasting *Prog. Org. Coat.* **123** 362–73
[14] Corsaro C, Orlando G, Costa G, Latino M, Barreca F, Mezzasalma A M, Neri F and Fazio E 2024 Wetting behavior driven by surface morphology changes induced by picosecond laser texturing *Materials* **17** 1–15
[15] Wang Q, Ma Y, Fu X, Liu M, Cao Z, Gai P and Zhou W 2024 Numerical simulation study of combined shot peening and laser shock peening on surface integrity of Ti-6Al-4V titanium alloy *Surf. Coat. Technol.* **487** 1–14
[16] Yıldıran Avcu Y, Yetik O, Koçoğlu H, Avcu E and Sınmazçelik T 2018 Dry sliding wear behaviour of shot peened TI6AL4V alloys at different peening times *Acta Phys. Pol.* A **134** 349–53
[17] Yildiran Avcu Y, Yetik O, Guney M, Iakovakis E, Sinmazcelik T and Avcu E 2020 Surface, subsurface and tribological properties of Ti6Al4V alloy shot peened under different parameters *Materials* **13** 1–22
[18] John M, Kalvala P R, Misra M and Menezes P L 2021 Peening techniques for surface modification: processes, properties, and applications *Materials* **14** 1–30
[19] Stolarik G, Nag A, Petru J, Svobodova J and Hloch S 2021 Ultrasonic pulsating water jet peening: influence of pressure and pattern strategy *Materials* **14** 1–17
[20] Stolárik G, Klichová D, Poloprudský J, Chlupová A, Nag A and Hloch S 2024 Submerged surface texturing of AISI 304L using the pulsating water jet method *Archives of Civil and Mechanical Engineering* **24** 1–21
[21] Srikanth M, Sai Charan B, Venu D M, Venkatesan K, Sreedhar G, Chattopadhyay K and Pattanayak D K 2025 Enhancement of high temperature oxidation and hot corrosion resistance behaviors of selective laser melted Ti6Al4V by ultrasonic shot peening *Mater. Chem. Phys.* **332** 1–14
[22] Si C, Song Z and Cao Y 2024 Effect of peening media type on the high-cycle tensile–tensile fatigue properties of Ti-6Al-4V alloy by ultrasonic shot peening *Fatigue & Fracture of Engineering Materials & Structures* **0** 1–17
[23] Wan L, Cai J, Qian Y, Wu S, Kang Y and Li D 2024 Surface integrity and fatigue performance of Ti6Al4V alloy peened by sinking bead abrasive jet *Journal of Materials Research and Technology* **32** 3169–80
[24] Soyama H, Wong K L, Eakins D and Korsunsky A M 2024 The effects of submerged laser peening, cavitation peening, and shot peening on the improvement of the torsional fatigue strength of powder bed fused Ti6Al4V produced through laser sintering *Int. J. Fatigue* **185** 1–17
[25] Zhang Y, Zhao X, Ren B, Wang H, Chen C, Liu Y and Hu C 2024 Wet shot peening effects on surface integrity and very high cycle fatigue of TC17 titanium alloy *Eng. Fail. Anal.* **166** 1–16
[26] Siahpour P, Amegadzie M Y, Moreau E D, Kalliecharan D, Monchesky T L, Tieu A, Christensen B, Donaldson I W and Plucknett K P 2022 Surface characteristics and residual stress generation in Ti-6Al-4 V following ultrasonic pulsed water jet peening *Surf. Coat. Technol.* **445** 1–18
[27] Poloprudsky J, Chlupova A, Sulak I, Kruml T and Hloch S 2021 Surface and subsurface analysis of stainless steel and titanium alloys exposed to ultrasonic pulsating water jet *Materials* **14** 1–20
[28] Husin H, Mat Nawi M N, Gebremariam M A, Saptaji K and Azhari A 2024 Experimental investigation on the effect of masked multiple passes abrasive waterjet machining surface texturing on coefficient of friction *Journal of Advanced Research in Applied Mechanics* **126** 138–48
[29] Stolárik G, Svobodová J, Klichová D, Nag A and Hloch S 2023 Titanium surface roughening with ultrasonic pulsating water jet *J. Manuf. Processes* **90** 341–56
[30] Hloch S, Srivastava M, Nag A, Müller M, Hromasová M, Svobodová J, Kruml T and Chlupová A 2020 Effect of pressure of pulsating water jet moving along stair trajectory on erosion depth, surface morphology and microhardness *Wear* **452-453** 1–16
[31] Zhang P, Yue X, Wang P and Zhai Y 2022 Influence of SiC pellets water jet peening on the surface integrity of 7075-T6 aluminum alloy *Vacuum* **196** 1–10
[32] Chakkravarthy V *et al* 2023 Effect of abrasive water jet peening on NaCl-induced hot corrosion behavior of Ti–6Al–4V *Vacuum* **210** 1–10
[33] Armağan M and Arıcı A A 2024 Analysis based on surface and kerf performance in multi-simultaneous cutting of S235JR structural steel with abrasive water jet *Machining Science and Technology* **28** 415–37
[34] Armağan M 2021 Cutting of St37 steel plates in stacked form with abrasive water jet *Mater. Manuf. Processes* **36** 1305–13
[35] Avcu E, Abakay E, Yıldıran Avcu Y, Çalım E, Gökalp İ, Iakovakis E, Koç F G, Yamanoglu R, Akıncı A and Guney M 2023 Corrosion behavior of shot-peened Ti6Al4V alloy produced via pressure-assisted sintering *Coatings* **13** 1–15
[36] Song F, Yao S, Liu L, Chi Y, Shao Z, Wang G, Jia Y, Zhang X and Tu S 2023 Submerged deflecting abrasive waterjet peening for improving the surface integrity and solid particle erosion resistance of Ti-6Al-4V alloy *Surface and Coatings Technology* **470** 1–12
[37] Hou R, zhang m, Wang Y and Lv Z 2022 *Research Square* (https://doi.org/10.21203/rs.3.rs-1578520/v1)

[38] Lv Z, Hou R, Wang R, Zhang Y and Zhang M 2022 Investigation on surface integrity and fatigue performance in abrasive waterjet peening *Journal of the Brazilian Society of Mechanical Sciences and Engineering* **44**

[39] Sadasivam B, Hizal A and Arola D 2009 Abrasive waterjet peening with elastic prestress: a parametric evaluation *Int. J. Mach. Tools Manuf.* **49** 134–41

[40] Soyama H and Sanders D 2019 Use of an abrasive water cavitating jet and peening process to improve the fatigue strength of titanium alloy 6Al-4V manufactured by the electron beam powder bed melting (EBPB) additive manufacturing method *JOM* **71** 4311–8

[41] Arola D, McCain M L, Kunaporn S R and M. Ramulu 2002 Waterjet and abrasive waterjet surface treatment of titanium: a comparison of surface texture and residual stress *Wear* **249** 943–50

[42] Wang G, Yao S, Chi Y, Zhang C, Wang N, Chen Y, Lu R, Li Z and Zhang X 2023 Improvement of titanium alloy TA19 fatigue life by submerged abrasive waterjet peening: correlation of its process parameters with surface integrity and fatigue performance *Chinese Journal of Aeronautics* **37** 377–90

[43] Dwayne M L M and Arola D 2000 *Abrasive Waterjet Peening: A New Method of Surface Preparation for Metal Orthopedic Implants* (Wiley)

[44] Arola D, Alade A E and Weber W 2006 Improving fatigue strength of metals using abrasive waterjet peening *Machining Science and Technology* **10** 197–218

[45] Lu S, Sun J, Ma Y and Sun N 2024 Pre-mixed abrasive waterjet peening with post-low stress milling process and the effect of process parameters on the surface integrity of TC11 titanium alloy *Surf. Coat. Technol.* **478** 1–26

[46] Yao S, Wang G, Li K, Wang N, Zhang C, Liu S, Liu C, Zhang X and Tu S 2022 Cavitation abrasive integrated waterjet peening process and the effect of process parameters on the surface integrity of TA19 titanium alloy *Surf. Coat. Technol.* **440** 1–13

[47] Wang G, Yao S, Chi Y, Zhang C, Wang N, Chen Y, Lu R, Li Z and Zhang X 2024 Improvement of titanium alloy TA19 fatigue life by submerged abrasive waterjet peening: correlation of its process parameters with surface integrity and fatigue performance *Chin. J. Aeronaut.* **37** 377–90

[48] Yao S-L, Li W, Wang J-S, Zeng F, Wang G-Y, Chi Y-X, Wang N, Liu S and Zhang X-C 2023 Surface strengthening in confined spaces: a novel deflecting abrasive waterjet peening for improving the surface integrity of nickel-based superalloys GH4169 *J. Manuf. Processes* **85** 417–33